

Available online at www.sciencedirect.com**ScienceDirect**

Energy Procedia 142 (2017) 501–506

Energy

Procediawww.elsevier.com/locate/procedia

9th International Conference on Applied Energy, ICAE2017, 21-24 August 2017, Cardiff, UK

A Microfluidic Reactor for Solar Fuel Production from Photocatalytic CO₂ Reduction

Evangelos Kalamaras^a, Mercedes Maroto-Valer^a, Jin Xuan^a, Huzhi Wang^{a*}^a*School of Engineering and Physical Sciences, Heriot-Watt University, Edinburgh, UK*

Abstract

Photocatalytic CO₂ conversion into usable chemical fuels is considered as an ideal way to tackle problems such as energy shortage and global warming simultaneously. In this “kill two birds with one stone” approach, CO₂ is used as feedstock and abundant solar light as energy source. For this purpose, a photocatalytic micro-reactor was designed in order to overcome problems of conventional photo-reactors including low surface-area-to-volume ratio, poor mass and photon transfer. Common materials such as Fluorine-doped Tin oxide (FTO) glass, Polymethyl methacrylate (PMMA) and surlyn that widely used in photoelectrochemical and solar cells were employed for the fabrication of the reactor. The feasibility and performance of the proposed reactor was tested in the challenging case of photocatalytic CO₂ reduction on TiO₂ thin film. The experimental results confirmed that one of the main products of CO₂ reduction was methanol. Maximum methanol concentration reached 162 μM at a flow rate of 120 μL/min.

© 2017 The Authors. Published by Elsevier Ltd.

Peer-review under responsibility of the scientific committee of the 9th International Conference on Applied Energy.

Keywords: CO₂ conversion; microfluidic; solar fuels; energy storage;

1. Introduction

Nowadays, global energy consumption is dominated by fossil fuels such as crude oil, natural gas and coal. However, fossil fuels are non-renewable which means that they are being depleted rapidly. Furthermore, combustion of conventional fuels is one of the most important factors of several environmental issues including global warming and greenhouse effect [1]. Therefore, there is an urgent need to use a renewable and environmentally friendly energy source to meet the energy demand of modern world. Among all clean energy sources, solar energy seems more

* Corresponding author. Tel.: +44 0 131 451 8354; fax: +44 0 131 451 3129.

E-mail address: h.wang@hw.ac.uk

attractive because it can cope with the current and the future energy needs [2]. Specifically, solar energy conversion into chemicals have been extensively investigated the last decades but there is a lot of room for improvements in order to achieve high efficiencies that will enable the commercialization of this technology.

Photocatalytic CO₂ reduction, which allows the direct conversion of CO₂ into chemicals, seems an ideal approach because it can address both environmental pollution and energy shortage at the same time. In this approach, CO₂ can be used as a raw material for the production of chemicals or usable fuels. Additionally, the produced fuels of this process can be transported and stored in the existing infrastructure systems. Photocatalytic CO₂ reduction process is also known as artificial photosynthesis because it mimics the natural process of plants that convert the atmospheric CO₂ into chemical products. A large variety of semiconductor-based photocatalysts has been studied for this modest goal since Inoue et al. in 1979 reported for the first time photoreduction of CO₂ into methanol, formaldehyde, formic acid and traces of methane using several photocatalysts including TiO₂, CdS, WO₃, ZnO, GaP and SiC [3].

Briefly, heterogeneous phototocatalytic CO₂ reduction can be summarized into the following steps:

- adsorption of CO₂ molecules on the surface of the photocatalyst,
- generation of electron-hole pairs through absorption of photons with energy equal to or higher than the band gap of the photocatalyst
- electron-hole separation and transportation
- reduction and oxidation reactions between the adsorbed species and the charge carriers on the surface.

Although many efforts have been done for the development of highly active semiconductor-based photocatalysts, CO₂ photo-conversion rates are still very poor. Apart from the performance of the photocatalyst, another important factor that plays a significant role in the efficiency of a photocatalytic CO₂ conversion system is the development of an effective photo-reactor. Specifically, mass transfer of CO₂, light distribution and specific surface area of photocatalyst to volume ratio highly depend on the photo-reactor design. Recently, new type of reactors have been introduced in photocatalytic applications known as optofluidic micro-reactors [4-7]. These reactors combine the advantages of microfluidics and optics providing fine flow control, high specific surface area to volume ratio, high light distribution and better light penetration compared to conventional photo-reactors.

In this study, the main objective was the design and fabrication of an optofluidic reactor that can be used not only for photocatalytic but also for photoelectrochemical CO₂ reduction. In photocatalytic CO₂ reduction experiments performed with this micro-reactor several products were obtained. However, only methanol was used to evaluate the photocatalytic performance of the reactor because it was one of the main products. Additionally, the effect of liquid flow rate on CO₂ conversion into methanol was investigated.

2. Experimental

2.1. Design and fabrication of microfluidic photo-reactor

A sandwich-type microfluidic photo-reactor was designed, as shown in fig. 1. FTO glasses were used as bottom and top layer. This type of glass was used not only for its transparency but also for its conductivity (Resistance 10 Ω/square) that will offer the possibility to use the same reactor for photoelectrochemical applications in the future. A PMMA layer (100 μm) was cut by Trotec Speedy 300 laser engraver/cutter. This PMMA layer was made in order to create a reaction chamber between the two FTO glasses. Finally, two gaskets of a thermoplastic film (Surlyn 30μm, Dyesol) were cut in laser cutter and placed between the PMMA layer and the FTO glasses sealing the reactor. Thus, the total volume of the micro-chamber was 32 μL (20 mm x 10 mm x 0.16 mm).

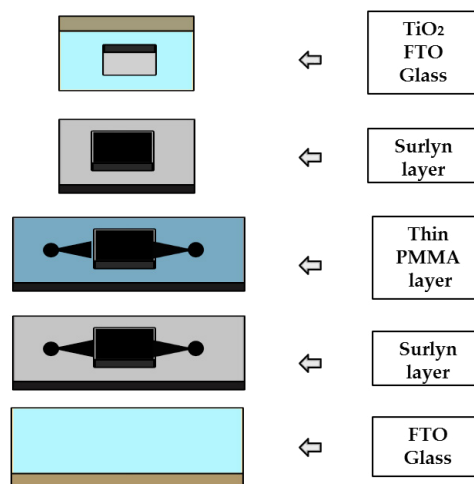


Fig. 1. Schematic representation of micro-reactor.

2.2. Fabrication of titania films

FTO transparent conductive electrodes were used as substrates for TiO₂ thin films. They were cut in the appropriate dimensions and were carefully cleaned by sonication sequentially in acetone, ethanol, and distilled water. TiO₂ thin films were fabricated using a nanoparticulate TiO₂ paste [8]. For the preparation of TiO₂ paste, 3 g of P25 Aeroxide[®] TiO₂ nanoparticles were dispersed in a solution containing 0.5 mL acetic acid and 1.5 mL distilled water. This dispersion was grinded in a mortar by adding 2 mL of ethanol. The last step was repeated for 20 times. After that, 10 g of terpineol and 1 g of ethyl cellulose solution (10% of ethyl cellulose diluted in ethanol) were added to this mixture and stirred vigorously for 1 h. Next, the ethanol was evaporated using a rotary evaporator device. The prepared paste was applied on FTO by doctor-blade technique. Finally, the samples were calcined at 550 °C for 10 min with temperature ramp of 10 degrees/min. The TiO₂ thin film (2 cm x 1 cm) was deposited in the centre of the FTO glass (3 cm x 2 cm).

2.3. Characterization methods

Thin films of TiO₂ were characterized by a UV/Vis spectrometer (Perkin Elmer Lambda 950) equipped with a 150 mm integration sphere (Perkin Elmer). Particle size of the TiO₂ thin films was observed with Focused Ion Beam (FIB) Emission Scanning Electron Microscopy (SEM, FEI Quanta 3D FEG). X-ray diffraction (XRD) patterns were observed on a D8 ADVANCE (Bruker AXS) diffractometer with Cu K α radiation and a nickel beta filter ($2\theta = 10\text{--}80^\circ$). CO₂ conversion into methanol was confirmed using Bruker AVIII 300MHz magnetic resonance (NMR) spectrometer.

2.4. Experimental configuration

The solution used for all the photocatalytic CO₂ reduction experiments was 0.5 M NaOH purged with high purity of CO₂ (99.99%) for 30 min. NaOH was chosen because liquid alkaline solutions have shown enhanced CO₂ solubility [9]. In addition, the presence of OH⁻ decrease the rates of electron-hole recombination because they act as hole scavengers. Pre-purged solution was supplied to micro-reactor by a syringe pump (Genie Touch, Kent Scientific Corporation). The liquid flow rate was in the range of 40 $\mu\text{L}/\text{min}$, 80 $\mu\text{L}/\text{min}$, 120 $\mu\text{L}/\text{min}$ and 200 $\mu\text{L}/\text{min}$. Next, the liquid solution was collected from the outlet and analyzed. In all experiments, Omnicure[®] S2000 spot UV curing lamp system was used as a UV light source. The light source was adjusted to emit 2 mW/cm² at 365 nm wavelength and confirmed by Omnicure[®] R2000 radiometer.

TiO₂ thin films were deposited on the FTO glass as already mentioned in subsection 2.2. The nanoparticulate mesoporous structure of TiO₂ can be clearly seen in the SEM image (fig. 2a). This structure stems from the aggregation of TiO₂ nanoparticles. In this particular case, (P25 Aerioxide®TiO₂) nanoparticles range from 20 to 30 nm and consist of a 75:25 ratio of anatase to rutile. The presence of both anatase and rutile phases was confirmed by the XRD patterns (fig.2b). Two different kinds of diffraction peaks were observed in XRD patterns corresponding to SnO₂ of FTO substrates and rutile and anatase phase of TiO₂ thin films. Strong diffraction peaks at 25° and 48° indicating TiO₂ in anatase phase, while diffraction peaks at 27°, 36° and 63° indicating TiO₂ in rutile phase. The calculated anatase and rutile crystallite sizes of TiO₂ thin films based on Scherrer equation are 20.7 and 34.4 nm, respectively. This is in good agreement with SEM images.

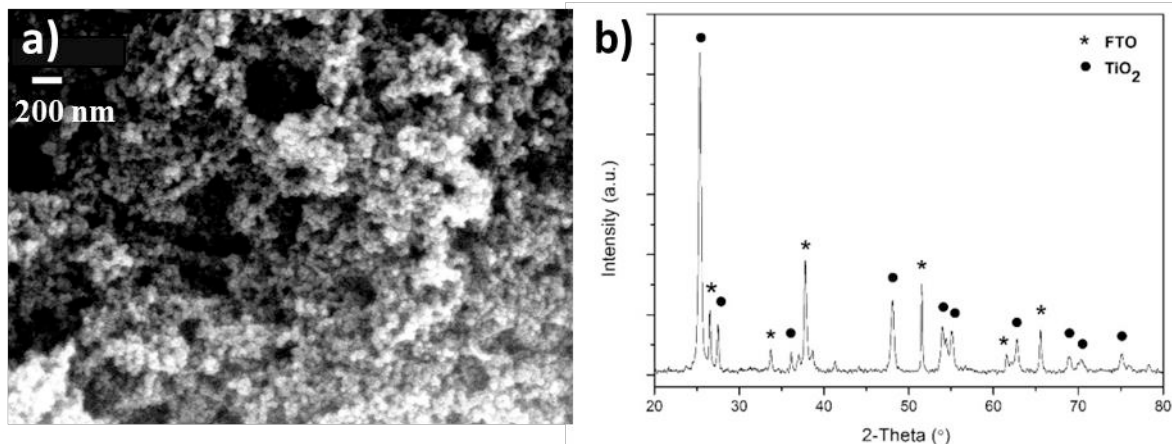


Fig. 2. a) SEM image of TiO₂ P-25 nanoparticulate film on FTO glass b) XRD pattern of TiO₂ thin film on FTO glass

Fig. 3 depicts the UV-Vis absorption spectra of nanoparticulate TiO₂ thin films. It can be easily seen that the absorption of these films is limited to only UV light region due to their large band gap. Specifically, the recorded spectral data showed a strong cut off at around 405 nm. In addition, the band gap of TiO₂ thin films was calculated to approximately 3.1 eV which is in good agreement with the literature [10].

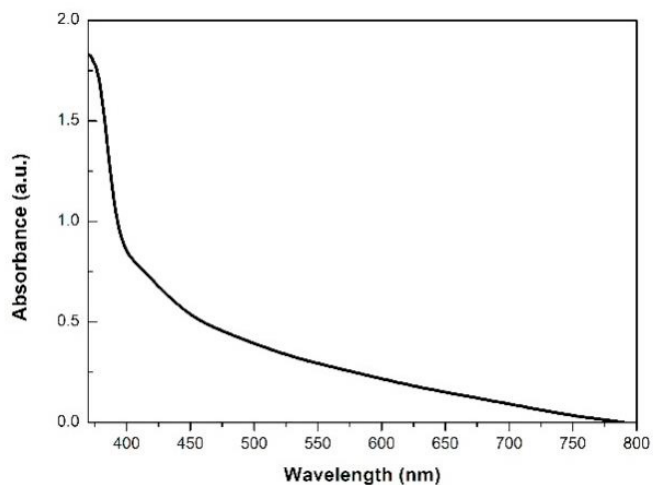


Fig. 3. UV-vis absorption spectra of TiO₂ P-25 nanoparticulate film on FTO glass

It has been reported that TiO₂ photocatalyst can convert CO₂ into several gas and liquid products. Consistent with these findings, several products were detected using ¹H NMR. Due to the fact that methanol was one of the main products, it was used for the evaluation of the performance of the micro-reactor. In all ¹H NMR experiments, a mixture of the collected solution and D₂O (4:1 volume ratio) was used. In fig. 4a, the peak showing a chemical shift of 3.32 ppm from the post-reaction solution matches very well with the methanol standard sample. To eliminate the possibility of any impurities pre-existing in the solution or inside the micro-chamber of photo-reactor, a pre-reaction solution was measured (fig. 4b). These ¹H-NMR spectra confirm the production of methanol through the photocatalytic CO₂ reduction route. The effect of liquid flow rate on the CO₂ photo-conversion into methanol was also investigated.

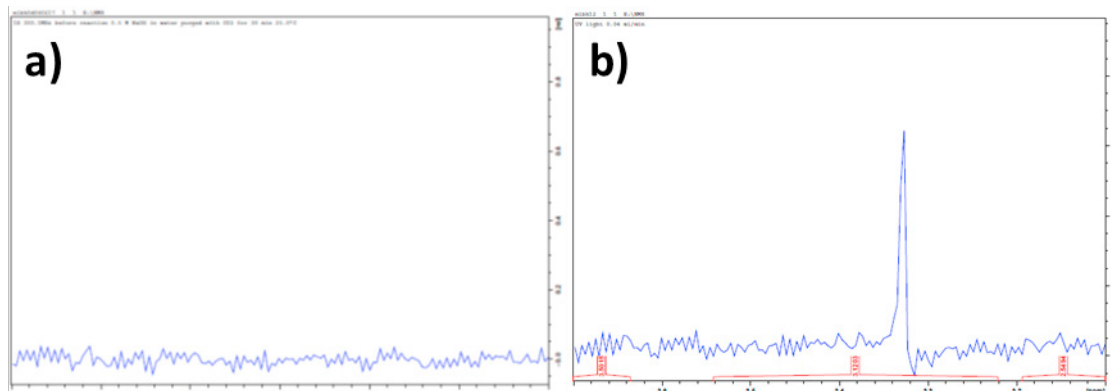


Fig. 4. ¹H-NMR spectra of a) pre-reaction and b) post-reaction solution.

¹H-NMR spectra confirm the production of methanol through the photocatalytic CO₂ reduction route. The effect of liquid flow rate on the CO₂ photo-conversion into methanol was also investigated. Quantification of product was also done through NMR analysis using dioxane as internal standard. The maximum methanol concentration was 162 μM at a flow rate of 120 μL/min. As it can be clearly seen in fig. 5, there is an optimal flow rate of approximately 120 μL/min resulting in the maximum methanol concentration.

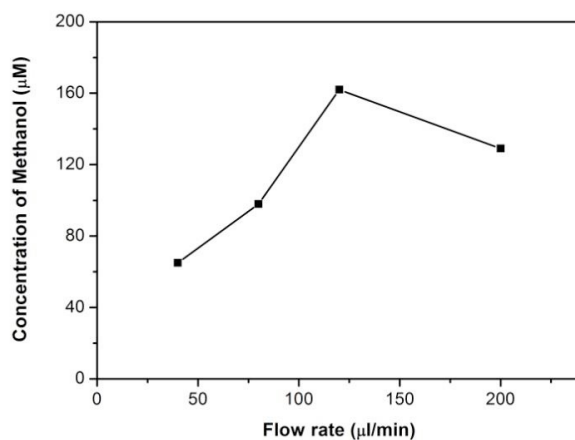


Fig. 5. Concentration of methanol vs flow rate.

Under low flow rates, less CO₂ is available to react on the surface of TiO₂ nanoparticles, while inefficient OH⁻ supply leads to a low hole-scavenging rate. In addition, large residence time, caused by low flow rate, can bring on

methanol photo-oxidation reaction on UV-illuminated TiO₂ thin films reducing significantly the CO₂ conversion rates. On the other hand, although mass transport was improved under high flow rates, reduced methanol concentration was observed due to the fact that CO₂ molecules were in contact with the TiO₂ nanoparticles for a shorter period of time [4].

4. Conclusions

The impact of the reactor design in photocatalytic and photoelectrocatalytic applications has not been studied in depth. In this study, we have showed the ability to convert CO₂ into methanol using a microfluidic micro-reactor. TiO₂, the “best-known material” in photocatalytic applications, was served as photocatalyst. Methanol was measured in order to check the feasibility and evaluate the performance of the photocatalytic micro-reactor. It was found that the optimal flow rate for this reactor was 120 μL/min resulting in 162 μM concentration of methanol in the solution. Further investigation to understand the significance of the microfluidic reactor design and the micro-chamber or micro-channel size is needed. It should be mentioned that the prepared reactor can offer the ability to explore the potential benefits of microfluidics in a large variety of applications using existing technology of photoelectrochemical cells without any further modification. Particularly, any kind of photocatalyst or electrocatalyst deposited on conductive substrates can be used in a continuous flow microfluidic reactor. In this way, the performance of existing photocatalytic or PEC systems can be increased due to improved mass transfer, better light distribution and higher specific surface area of catalyst to volume ratio. Finally, continuous flow microfluidic reactors can assist to provide a better understanding of the photocatalytic mechanism of reactions such as CO₂ reduction.

Acknowledgements

This research was supported by the Heriot-Watt University Start-up Fund.

References

- [1] M. Mikkelsen, M. Jorgensen, F.C. Krebs, The teraton challenge. A review of fixation and transformation of carbon dioxide, *Energy Environ. Sci.*, 3 (2010) 43-81.
- [2] G. Centi, S. Perathoner, Towards Solar Fuels from Water and CO₂, *ChemSusChem*, 3 (2010) 195-208.
- [3] T. Inoue, A. Fujishima, S. Konishi, K. Honda, Photoelectrocatalytic reduction of carbon dioxide in aqueous suspensions of semiconductor powders, *Nature*, 277 (1979) 637-638.
- [4] X. Cheng, R. Chen, X. Zhu, Q. Liao, L. An, D. Ye, X. He, S. Li, L. Li, An optofluidic planar microreactor for photocatalytic reduction of CO₂ in alkaline environment, *Energy*, 120 (2017) 276-282.
- [5] X. Cheng, R. Chen, X. Zhu, Q. Liao, X. He, S. Li, L. Li, Optofluidic membrane microreactor for photocatalytic reduction of CO₂, *International Journal of Hydrogen Energy*, 41 (2016) 2457-2465.
- [6] R. Chen, X. Cheng, X. Zhu, Q. Liao, L. An, D. Ye, X. He, Z. Wang, High-performance optofluidic membrane microreactor with a mesoporous CdS/TiO₂/SBA-15@carbon paper composite membrane for the CO₂ photoreduction, *Chem. Eng. J.*, 316 (2017) 911-918.
- [7] J. Parmar, S. Jang, L. Soler, D.-P. Kim, S. Sanchez, Nano-photocatalysts in microfluidics, energy conversion and environmental applications, *Lab on a Chip*, 15 (2015) 2352-2356.
- [8] S. Ito, P. Chen, P. Comte, M.K. Nazeeruddin, P. Liska, P. Péchy, M. Grätzel, Fabrication of screen-printing pastes from TiO₂ powders for dye-sensitised solar cells, *Progress in Photovoltaics: Research and Applications*, 15 (2007) 603-612.
- [9] J.A. Vega, W.E. Mustain, Effect of CO₂, HCO₃⁻ and CO₃⁻² on oxygen reduction in anion exchange membrane fuel cells, *Electrochim. Acta*, 55 (2010) 1638-1644.
- [10] R. López, R. Gómez, Band-gap energy estimation from diffuse reflectance measurements on sol-gel and commercial TiO₂: a comparative study, *Journal of Sol-Gel Science and Technology*, 61 (2012) 1-7.